

Spontaneous Self-Assembly of Fully Protected Ester 1:1 [α/α -N ^{α} -Bn-hydrazino] Pseudodipeptides into a Twisted Parallel β -Sheet in the Crystal State

Eugénie Romero,[†] Ralph-Olivier Moussodia,[†] Alexandre Kriznik,[‡] Emmanuel Wenger,[§] Samir Acherar,^{*†} and Brigitte Jamart-Grégoire^{*†}

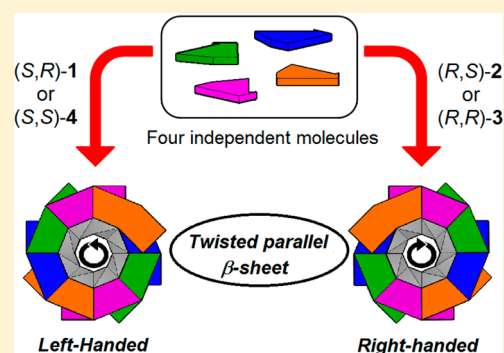
[†]Laboratoire de Chimie Physique Macromoléculaire (LCPM), Université de Lorraine-CNRS, UMR 7375, 1 rue Grandville, BP 20451, 54001 Nancy cedex, France

[‡]Ingénierie Moléculaire et Physiopathologie Articulaire (IMoPA), Université de Lorraine-CNRS, UMR 7365 and Service Commun de Biophysique Interactions Moléculaires (SCBIM), Université de Lorraine, FR3209, Biopôle de l'Université de Lorraine, Campus Biologie Santé – Faculté de Médecine, 9 Avenue de la Forêt de Haye, CS 50184, 54505 Vandœuvre-lès-Nancy, France

[§]Laboratoire de Crystallographie, Résonance Magnétique et Modélisations (CRM2), Université de Lorraine-CNRS, UMR 7036, Faculté des Sciences et Technologies, BP 70239, Boulevard des Aiguillettes, 54506 Vandœuvre-lès-Nancy cedex, France

Supporting Information

ABSTRACT: Previous studies have demonstrated that amidic α/β -pseudodipeptides, 1:1 [α/α -N ^{α} -Bn-hydrazino], have the ability to fold via a succession of γ -turn (C_7 pseudocycle) and hydrazinoturn in CDCl₃ solution, their amide terminals enabling the formation of an intramolecular H-bond network. Despite their lack of a primary amide terminals allowing the formation of the hydrazinoturn, their ester counterparts **1–4** were proven to self-assemble into C_6 and C_7 pseudocycles by intramolecular H-bonds in solution state and into an uncommon twisted parallel β -sheet through intermolecular H-bonding in the crystal state to form a supramolecular helix, with eight molecules needed to complete a full 360° rotation. Such self-organization (with eight molecules) has only been observed in a specific α/α -pseudodipeptide, depsipeptide (Boc-Leu-Lac-OEt). Relying on IR absorption, NMR, X-ray diffraction, and CD analyses, the aim of this study was to demonstrate that stereoisomers of ester 1:1 [α/α -N ^{α} -Bn-hydrazino] pseudodipeptides **1–4** are able to self-assemble into this β -helical structure. The absolute configuration of the asymmetric C ^{α} -atom of the α -amino acid residue influences the left- or right-handed twist without changing the pitch of the formed helix.



INTRODUCTION

By definition, molecular self-assembly is the spontaneous organization of individual molecules without external guidance into structurally well-defined and rather stable arrangements through a number of noncovalent interactions.¹ Many crucial biological functions rely on the ability of peptides to display particular folding/self-assembly patterns or secondary structures, called helices, turns, and β -sheets, which occur through the formation of H-bonds established between α -amino acid backbone atoms. Among the various secondary structures, the β -sheet family, also called β -pleated sheet (Figure 1), is the less well studied for small-molecule structures. Their relative lack of study, compared to that of α -helices, can be considered quite surprising because the formation of supramolecular β -sheet architectures is at the basis of various neurodegenerative diseases such as Alzheimer's,² Huntington's,³ prion protein,⁴ and other related diseases.⁵

The use of peptides in biological applications such as drug delivery is severely hampered by their inherent propensity to rapid degradation through proteolysis. As an alternative,

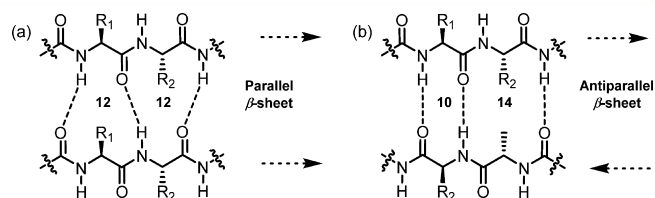


Figure 1. Hydrogen bond patterns in β -sheets: (a) parallel β -sheet (C_{12} pseudocycles) and (b) antiparallel β -sheet (C_{14} and C_{10} pseudocycles). The dotted arrows represent the direction of the peptide chain.

biologically active pseudopeptides, i.e. peptides with modified backbones, have emerged due to their potential resistance to peptidases and proteases and their ability to adopt well-defined secondary structures similar to their corresponding peptide analogues.⁶ Gellman and Seebach^{7,8} have demonstrated that β -

Received: July 13, 2016

Published: September 14, 2016

peptides (Figure 2) were able to adopt well-defined arrangement and to display stability against proteases and peptidases.⁹

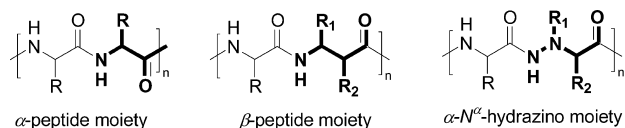


Figure 2. Backbones of α -peptide, β -peptide, and α - N^{α} -hydrazino moieties.

These pioneering studies have paved the way to the intensive studies of linear and cyclic β -peptides,^{7–9} hybrid pseudopeptides consisting of α/β -, α/γ -, and β/γ -amino acids,¹⁰ together with the less common studies of β/δ - and γ/δ -pseudopeptides.¹¹ The use of heterogeneous backbones in pseudopeptidic designs was indeed justified by studies in the 2000s indicating the relevance of the introduction of a β -amino acid in a peptide to both increase the proteolysis stability¹² and induce a preorganization that could lead to new folding possibilities.^{10c}

Extending the β -peptide concept has given birth to bis-nitrogenated compounds in which the C^{β} -atom has been replaced by a nitrogen atom, leading to the new family of “hydrazinopeptides”.¹³ Previous studies performed in our laboratory have demonstrated the ability of mixed amidic 1:1 [α/α - N^{α} -hydrazino]mers to self-assemble via a succession of γ -turn (C_7 pseudocycle) and hydrazinoturn (Figure 3). The latter

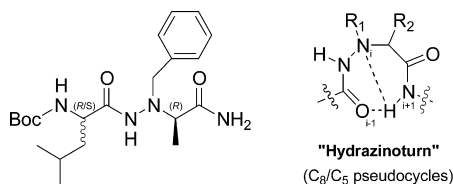


Figure 3. Self-organization of amidic 1:1[leucine/ α - N^{α} -Bn-(D)-hydrazinoalanine] pseudodipeptides through the “hydrazinoturn”. C_5 is $N_{i+1}-H \cdots N_i$ and C_8 is $N_{i+1}-H \cdots O_{i-1}=C$ intramolecularly H-bonded.

consists of the formation of a bifurcated hydrogen bond through C_5 and C_8 pseudocycles, involving the lone pair of the N^{α} -atom. Interestingly, this specific intramolecular H-bond network is formed regardless of the chirality.¹⁴ Moreover, cyclization of mixed 1:1 [α/α - N^{α} -hydrazino]mers led to the corresponding macrocycles which were able to self-assemble into nanotubes via the formation of an intermolecular H-bond network.¹⁵

Such versatile self-organization, i.e. succession of γ -turn and hydrazinoturn, emphasized the particular role of the hydrazino link within this pseudopeptide series. These results led us to envision the possibility to access to various secondary structures by wisely manipulating this particular backbone.

As currently employed to simulate the role of the amide bond in protein folding, we decided to replace the amide terminals by an ester through “amide-to-ester mutagenesis”,¹⁶ thereby preventing our newly formed ester 1:1 [α/α - N^{α} -Bn-hydrazino] pseudodipeptide from folding into a hydrazinoturn. We propose that this backbone modification should open the door to new “intermolecular” self-assemblies promoted by the intrinsic preorganization of the hydrazinopeptides.¹⁷

In this study, we thus undertook the synthesis and the conformational analysis of ester 1:1 [α/α - N^{α} -Bn-hydrazino]

pseudodipeptides 1–4 (Figure 4). To evaluate the influence of the chirality on the structuration, we decided to compare the

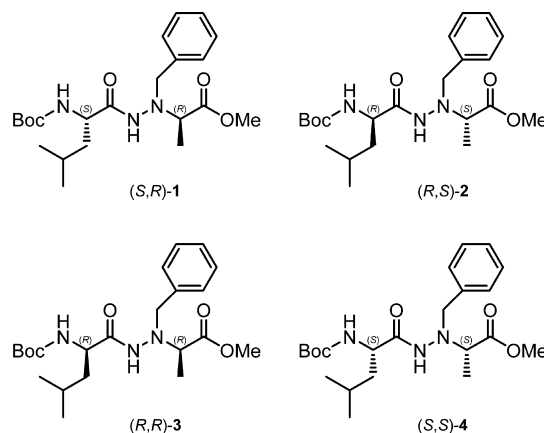


Figure 4. Chemical structures of the stereoisomers of ester 1:1[α/α - N^{α} -Bn-hydrazino] pseudodipeptides 1–4.

structuration of enantiomers (S,R)-1 and (R,S)-2, or (R,R)-3 and (S,S)-4 respectively. It is important to note that compounds 1–4 possess an sp^3 nitrogen atom (N^{α} -atom) which can be considered as an extra chiral center with a nonfixed configuration. The conformational analyses in solution and in solid state will be studied by using X-ray crystallography, microcrystalline CD, NMR, and IR data.

RESULTS AND DISCUSSION

Studies of the Self-Assembly in Solution State by 1H NMR Experiments and FTIR Absorption Spectroscopy.

Ester [α/α - N^{α} -hydrazino] pseudodipeptides 1–4 were synthesized according to our previously described procedure.¹⁴ In a first step, the conformation of the stereoisomers 1–4 in solution state was studied through 1H NMR and FTIR absorption techniques. First of all, we showed that no significant differences could be pointed out when comparing the spectra of compounds 1–4 (see Supporting Information pp S2 to S9). The data obtained for compound (S,R)-1 are described below as a reference.

1H NMR spectra were recorded in $CDCl_3$ in a range of concentration varying from 10^{-4} to 10^{-1} M. No significant variation was observed (Figure 5a) concerning the chemical shifts of the carbamidic (NHBoc) and hydrazidic NH protons. This result demonstrated that no intermolecular H-bonding occurs in compound (S,R)-1. On the basis of small model compounds described in one of our earlier studies,^{18f} we established that the chemical shifts of non-H-bonded carbamic and hydrazidic NH protons are estimated to be roughly 4.7 and 6.5 ppm, respectively. Taking into account these data, the carbamidic NH proton of compound (S,R)-1 located at 4.8 ppm has been considered as a non-H-bonded proton. On the contrary, the hydrazidic proton located at 8.0 ppm (instead of 6.5 ppm for free one) has been defined as a H-bonded proton.

To validate these assumptions, 1H NMR spectra were also recorded in a mixture of $CDCl_3/DMSO-d_6$ ($c = 10^{-2}$ M, from 0 up to 10%, Figure 5b) to detect the NH protons involved in an intramolecular H-bond. Solvents with H-bond acceptor atoms, such as $DMSO-d_6$, are able to form intermolecular H-bonds producing a downfield shift, which is less significant when the H atom participates in an intramolecular H-bond. This type of experiment has been proven to be efficient in evaluating the H-

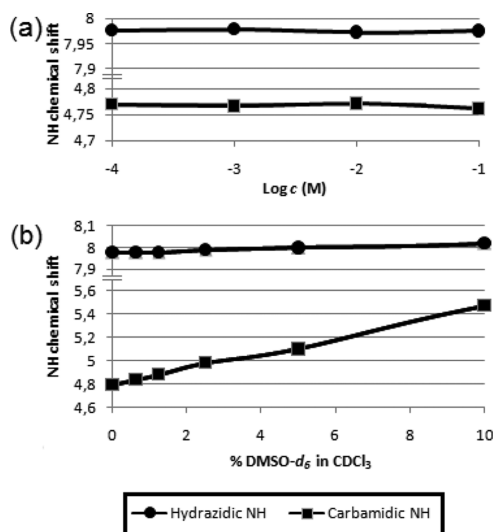


Figure 5. (a) Concentration dependence in CDCl₃ (from 10⁻⁴ to 10⁻¹ M) and (b) solvent dependence as determined by ¹H NMR (300 MHz) in mixed CDCl₃/DMSO-*d*₆ (c = 10⁻² M) of NH chemical shifts of 1.

bond strength.¹⁸ As shown in Figure 5b, the chemical shift of the hydrazidic NH proton is unchanged whatever the amount of DMSO, which means that it is involved in an intramolecular H-bond. Conversely, the chemical shift of the free carbamidic NH proton (NHBoc) is sensitive to DMSO.

Careful inspection of the ¹H and ¹³C NMR spectra of compound (*S,R*)-1 (see Supporting Information pp S2 to S5) revealed an additional minor set of signals, demonstrating the presence of several conformations in CDCl₃ solution. These various conformations were due to the possible presence of *E/Z* isomerism of the hydrazidic bond^{18f,19} and leucine side-chain rotamers.²⁰ At this point, two possible conformations (C₆ and C₇ pseudocycles), involving the hydrazidic NH proton, were envisioned (Figure 6).

To complement these NMR results, FTIR absorption spectroscopic studies were also conducted. FTIR absorption spectroscopy is an efficient method to detect several conformers in solution by giving differentiable N–H and C=O signals for each conformer.²¹ FTIR experiments were

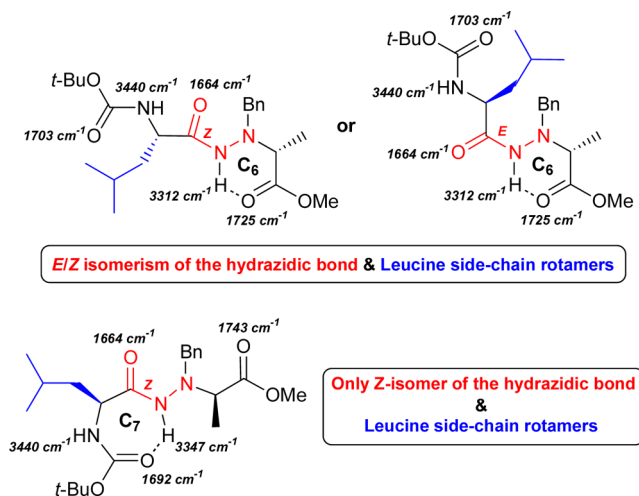


Figure 6. Possible conformations of compound 1 in CDCl₃ solution.

conducted in CDCl₃ at a concentration where intermolecular contacts have been experimentally proved to be undetectable (c = 10⁻² M).

Figure 7 presents the IR spectra of N–H and C=O stretching regions of compound (*S,R*)-1 (three and five bands,

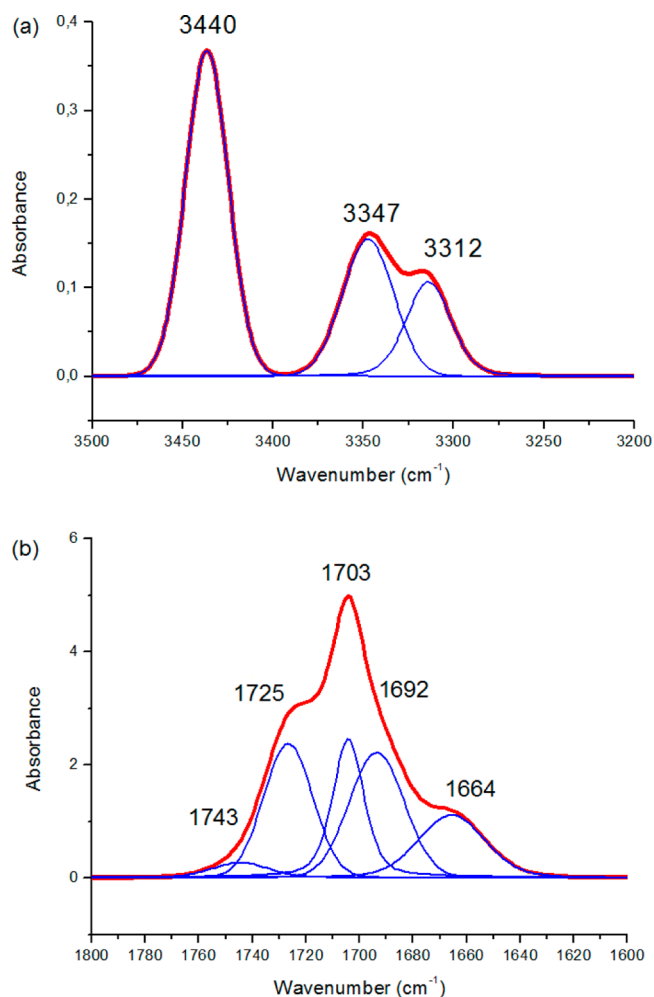


Figure 7. IR spectra (in red) and deconvoluted IR spectra (in blue) of (a) N–H and (b) C=O stretching regions in CDCl₃ (c = 10⁻² M) of 1.

respectively). For the N–H stretching region, the first band at 3440 cm⁻¹, located in the free N–H domain (>3400 cm⁻¹),^{17,21} corresponds to the free NHBoc and the two other bands at 3347 and 3312 cm⁻¹ were assigned to the H-bonded hydrazidic NH which is involved in both conformations described above (Figure 6). Among the 5 bands observed in the C=O domain, 4 bands (1743/1725 cm⁻¹ and 1703/1692 cm⁻¹) were assigned to the ester and carbamidic CO (free/bonded), respectively, and the last one located at 1664 cm⁻¹ to the free hydrazidic CO, which is not involved in any intramolecular H-bond. These FTIR absorption results are an endorsement of our hypothesis that compound (*S,R*)-1 adopts both C₆ and C₇ conformations in CDCl₃ solution (Figure 6).

The same kind of FTIR absorption analysis is obtained at high concentration (c = 1 M, CDCl₃), indicating that this conformational equilibrium is still maintained. It is noteworthy that the same self-organization has been observed in other solvents (c = 10⁻² M) such as toluene and methanol (see Supporting Information pp S10 and S11).

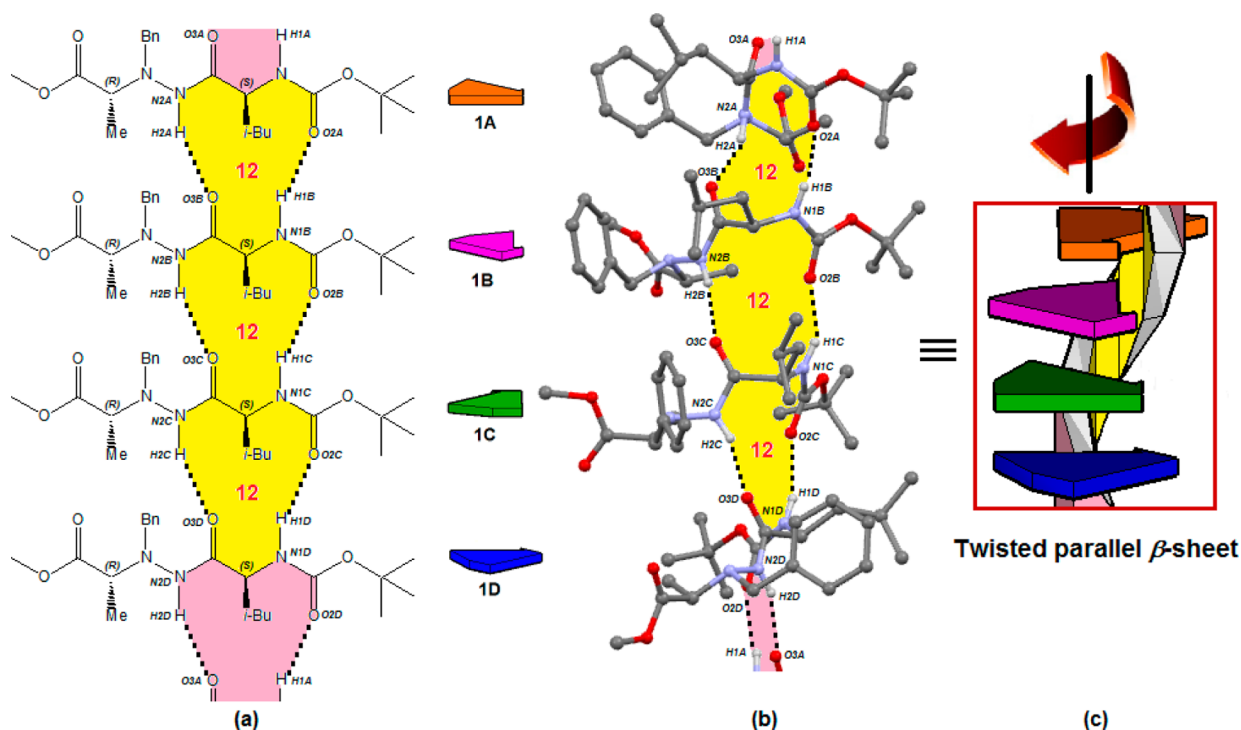


Figure 8. (a) Hydrogen bond patterns between four independent molecules (1A–1D), (b) 12-membered hydrogen-bonded rings, and (c) cartoon representation of the twisted parallel β -sheet for **1**.

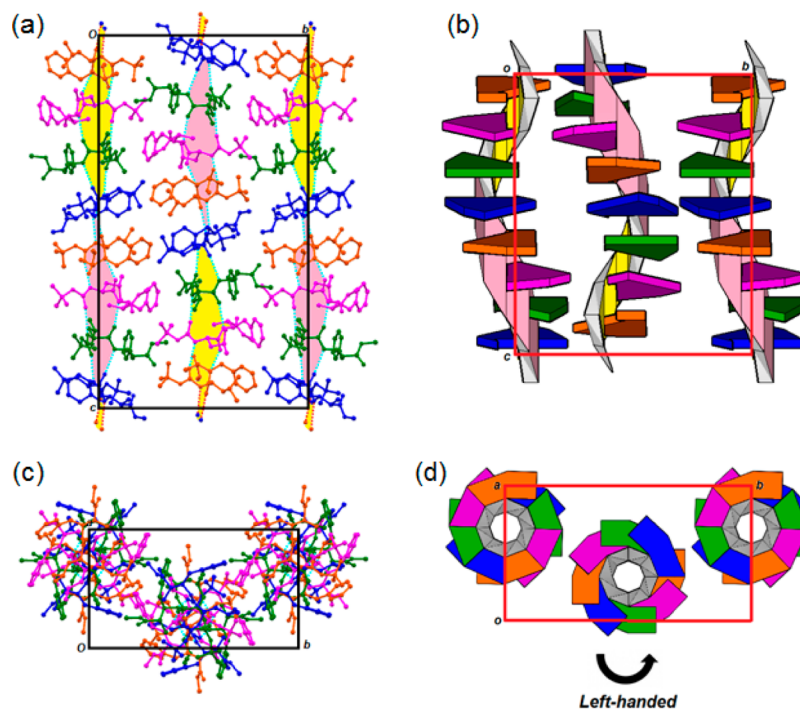


Figure 9. (a, c) Molecular packing and (b, d) cartoon representation of the twisted parallel β -sheet of **1** viewed along the *a* and *c* axis, respectively.

Studies of the Self-Assembly of 1–4 in the Crystal State by X-ray Diffraction. Crystals of compounds **1–4** were grown by slow evaporation from a dichloromethane/petroleum ether solution and crystallized in the space group $P2_12_12_1$ (see [Supporting Information](#) pp S12 to S23 for more details). Crystallographic data and structure refinement parameters are reported in CIF format with CCDC references 1447540 to 1447543 (a copy of CIF formats are available in [Supporting](#)

[Information](#)). The crystal structure determination of (*S,R*)-**1** and (*R,S*)-**2** was obtained from low-resolution X-ray diffraction data collected at 100 K (*R*-factor values of 6.92% and 9.56%, respectively). Regarding compounds (*R,R*)-**3** and (*S,S*)-**4**, poor X-ray diffraction data were collected (*R*-factor values of 17.04% and 12.14%, respectively). Consequently, their crystal structures are less resolved but are still sufficient to confirm the packing and the folding.

The X-ray diffraction structure of the heterochiral ester (S,R)-1 corresponds to 16 molecules in the unit cell (four molecules 1A–1D in the asymmetric unit), and the N^α-atom has a pyramidal conformation with (S)-configuration (Figures 8 and 9). The four independent molecules 1A–1D stacked one atop the other form a tetramer block, and two of these can interact together to provide an octamer block. This tetrameric/octameric association is maintained through an intermolecular H-bonding network between the carbamidic C=O and NH and the hydrazidic C=O and NH of each molecule 1A–1D, closing a 12-membered H-bonded pseudocycle with a distance $d_{(C=O \cdots H-N)}$ of 1.98 to 2.16 Å (Figures 8, 9 and Table S2 in Supporting Information), demonstrating a parallel β -sheet arrangement as indicated in Figure 1.

The data collected from the crystal analysis of the intermolecular packing clearly show no intramolecular H-bonds in the crystal lattice, as evidenced by the high nuclear distances. The “ β -strand” molecules stack up on top of each other into a parallel fashion through intermolecular H-bonds. However, the most interesting feature of this self-assembly is the presence of a twist that shapes a left-handed helical supramolecular structure. The formation of a helical structure will be referred to as a twisted β -sheet. It is noteworthy that the formed helix requires eight molecules to complete a full 360° rotation with a pitch of 38.20 Å. In the CCDC database, there are various examples of acyclic dipeptides with parallel β -sheet structures²² (flat tapes or twisted with different numbers of molecules per turn), but only one parallel twisted β -sheet was observed with eight molecules per turn (depsidipeptide Boc-Leu-Lac-OEt).²³

By taking a close look at the torsion angle values (ω , ϕ , and ψ) of the Leu residue, responsible for the left-handed helical supramolecular structure, we have found that these values are closely related to the left-handed type-II poly(L-Pro)_n conformation (Table 1),²⁴ but the supramolecular helix is approximately four times more elongated than type II poly(L-Pro)_n helix by comparing their helical pitch (Table 1).

Table 1. Selected Parameters Characterizing the Left-Handed Helical Supramolecular Structure in 1 and the Left-Handed Type-II Poly(L-Pro)_n Helix

	supramolecular helix in 1	type-II poly(L-Pro) _n helix ²⁴
ω (deg)	+172 to +180	+180
ϕ (deg)	−81 to −70	−80
ψ (deg)	+115 to +124	+150
n	8 ^a	3 ^b
pitch (Å)	38.20	9.3

^aNumber of residues (L-Pro) per helical turn for the type-II poly(L-Pro)_n helix. ^bNumber of molecules per helical turn for the supramolecular helix in 1.

X-ray diffraction analysis of compound (R,S)-2 showed that changing the α -carbon chirality of both the α -amino acid and the α -N^α-Bn-hydrazino acid residues in our pseudodipeptide backbone reverses the chirality of the N^α-atom. As a result, the corresponding heterochiral (R,S)-2 is the enantiomer of (S,R)-1 and logically leads to a reverse turn of the β -helical structure, i.e. compound (R,S)-2 adopts a right-handed twist with the same helical pitch (38.19 Å, Figure 10). It is known that an achiral pseudodipeptide (CCDC refcode XEZDUC) is able to form a parallel twisted β -sheet self-assembly.²⁵ However, as compounds 1 and 2 possess two chiral carbons, we decided to

analyze the crystal structures of homochiral (R,R)-3 and (S,S)-4 stereoisomers to know which chiral carbon was responsible for the control of helicity. The results were unambiguous and are presented in Table 2.

Homochiral compounds (R,R)-3 and (S,S)-4 (see Supporting Information pp S19 to S24) present the same kind of β -helical structures as those observed with heterochiral compounds with a left- and right-handed twist, respectively. The crystal structure of (R,R)-3 corresponds to 16 molecules in the unit cell (four molecules of 3A–3D in the asymmetric unit) with the N^α-atom having a pyramidal conformation with (R)-configuration as observed for (R,S)-2. As previously, the chirality inversion of N^α-atom between (R,R)-3 and (S,S)-4 occurred, making them an enantiomeric couple, with a N^α-atom adopting the same configuration as the C^α-atom of the α -amino acid residue. Therefore, this alternating switch of the helicity, without changing the helical pitch, can undoubtedly be attributed to the α -carbon chirality of the α -amino acid residue by comparison of the crystal structures of stereoisomers 1–4.

Indeed, a careful consideration of the intermolecular H-bond network points out that only one of the two asymmetric carbons present in the 1:1 [α/α -N^α-Bn-hydrazino] pseudodipeptide backbone, namely the α -amino acid C^α, is involved in the formation of the 12-membered H-bond pseudocycle responsible for the parallel β -sheet formation (Figure 9). This seems to pinpoint the fact that a D-amino acid in the ester 1:1 [α/α -N^α-Bn-hydrazino] pseudodipeptide series will induce a right-handed twisted β -sheet, while its L-amino acid counterpart will lead to a left-handed helical structure.

Studies of the Self-Assembly of 1–4 in the Crystal State by Microcrystalline Circular Dichroism. CD spectroscopy has been widely used to investigate structural changes in nonracemic chiral organic molecules. While it is frequently performed in solution, solid-state CD analysis, through the microcrystalline technique, also represents a powerful tool that provides crucial specific supramolecular information.²⁶ CD spectra were recorded on microcrystals of compounds 1–4 obtained by crushing the crystals in a mortar.

With the aim of optimizing results, microcrystals of 1–4 were suspended in Nujol oil ($c = 25\text{--}50 \text{ mg}\cdot\text{mL}^{-1}$), which is required to achieve a viscous suspension. Figure 11 depicts microcrystalline CD spectra of compounds 1–4, and it is worth mentioning that Nujol oil has no effect on the CD signal.

As illustrated in Figure 11, the shape of CD curves differs from those conventionally used for the determination of protein secondary structure (α -helix, β -sheet or random coil)²⁷ and provides a specific signal for both homochiral and heterochiral series. In each series, we clearly observed an inversion of the CD signal, which confirms the presence of two pairs of enantiomers as well as the complete chirality control of the N^α-atom in the crystal state.

In the homochiral series (Figure 11a), compound (R,R)-3 presents, contrary to its enantiomer (S,S)-4, only one broad positive band centered at approximately 233 nm, and two negative bands estimated at 217 and 198 nm. Analysis of heterochiral series gives too weak signals when recorded on a CD spectropolarimeter. By the fact, CD spectra of compounds 1 and 2 were recorded on a SRCD (synchrotron radiation CD) spectropolarimeter. By correlating the X-ray diffraction and CD results of (R,R)-3 and (S,S)-4, we can conclude that the shape of the curves of (R,R)-3 and (S,S)-4 refer to right- and left-handed helical β -sheet structures, respectively.

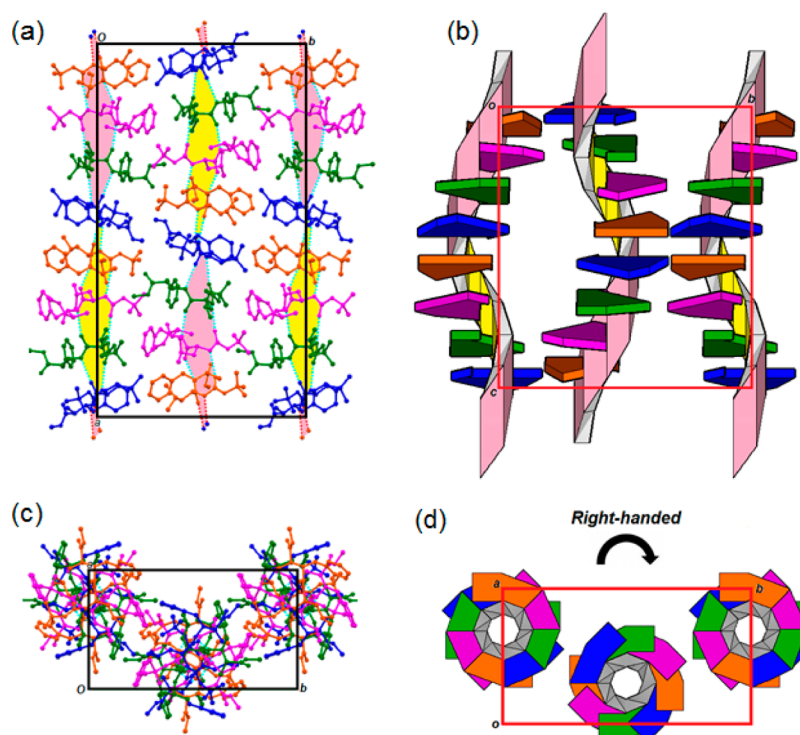


Figure 10. (a, c) Molecular packing and (b, d) cartoon representation of the twisted parallel β -sheet of **2** viewed along the a and c axis, respectively.

Table 2. Summary of the Handedness of the Helices Adopted by 1–4 in the Crystal State

compound	chirality of the N^α -atom	twist direction of the helix	pitch (Å)
(<i>S,R</i>)- 1	<i>S</i>	left-handed	38.20
(<i>R,S</i>)- 2	<i>R</i>	right-handed	38.19
(<i>R,R</i>)- 3	<i>R</i>	right-handed	38.17
(<i>S,S</i>)- 4	<i>S</i>	left-handed	38.21

To support these conclusions, compounds **5** and **6**¹³ (Figure 12) were analyzed by microcrystalline CD. Pseudodipeptide **5** is an analogue of (*S,R*)-**1** and of (*R,R*)-**3** bearing a glycine residue (no chiral carbon center) instead of the leucine one. Compound **6** is a C-terminal amide analogue of (*S,R*)-**1** and is known to fold via an hydrazinoturn which could prevent the self-assembly into β -sheets.

Crystals of compounds **5** and **6** were grown by slow evaporation from a dichloromethane/petroleum ether mixture, but once again the poor quality crystals prevented us from performing the X-ray diffraction analysis. However, as noted earlier, the microcrystalline CD spectra of these compounds could be recorded on a CD spectrometer (Figure 13).

CD spectra of compounds **5** (Figure 13a) and **6** (Figure 13b) are close to those of aryl benzyl sulfoxide compounds, presenting only a particular negative maximum value around 230 nm corresponding to the benzyl part.²⁸ This observation suggests that the presence of a new hydrogen bond donor site at the C-terminal position (compound **6**) and the absence of a chiral carbon center in the α -amino acid residue (compound **5**) avoid the supramolecular self-assembly into β -sheets. In the case of **6**, it possibly due to a bifurcated intramolecular H-bond (called hydrazinoturn), as was previously demonstrated in the CDCl_3 solution state.¹⁴

CONCLUSION

In summary, we highlighted in this work that fully protected 1:1 [α/α - N^α -Bn-hydrazino] pseudodipeptides **1–4** can self-assemble in a twisted β -sheet supramolecular structure in the crystal state. The N^α atom chirality is fixed and adopts the same configuration as the C^α -atom of the α -amino acid residue. Changing the chirality of the C^α -atom of the leucine residue leads to the inversion of the helicity of the twisted β -sheet, without changing the helical pitch. Finally, this supramolecular β -helical structure is not maintained in the solution state, leaving in its place a conformational equilibrium between C_6 and C_7 pseudocycles.

The study of the morphology of pseudodipeptides **1–4** by SEM analyses to determine if these pseudodipeptides can generate any amyloid-like fibrils through β -sheet mediated self-assembly, which is a main cause of the neurodegenerative disease Alzheimer's, is currently in progress.

EXPERIMENTAL SECTION

NMR. All NMR spectra (1D and 2D) were recorded at 298 K on a 300 MHz spectrometer with tetramethylsilane (TMS) as the internal standard. Chemical shifts (δ) are reported in ppm downfield from CDCl_3 ($\delta = 7.26$ ppm) for ^1H NMR and relative to the central CDCl_3 resonance ($\delta = 77.0$ ppm) for ^{13}C NMR spectroscopy. ^{13}C multiplicity data were obtained from JMOD experiments (C and CH_2 up, CH_3 and CH down). For ^1H NMR spectroscopic data, the coupling constants (J) are given in hertz and the multiplicity is defined as s for singlet, d for doublet, q for quartet, m for multiplet, br for broad, or combinations thereof. ^1H and ^{13}C NMR signals were assigned with the help of COSY, ROESY, JMOD, HSQC, and HMBC experiments.

For each compound, ^1H and ^{13}C NMR data indicated the presence of multiple conformations in CDCl_3 solution due in large part to the *E/Z* isomerism of the hydrazidic bond¹⁹ and/or the possible rotamers of the leucine side chain.²⁰ Only the chemical shifts of the major conformations are given. Owing to the similarity of the ^1H and ^{13}C NMR spectra, only one characterization data is given for each pair of

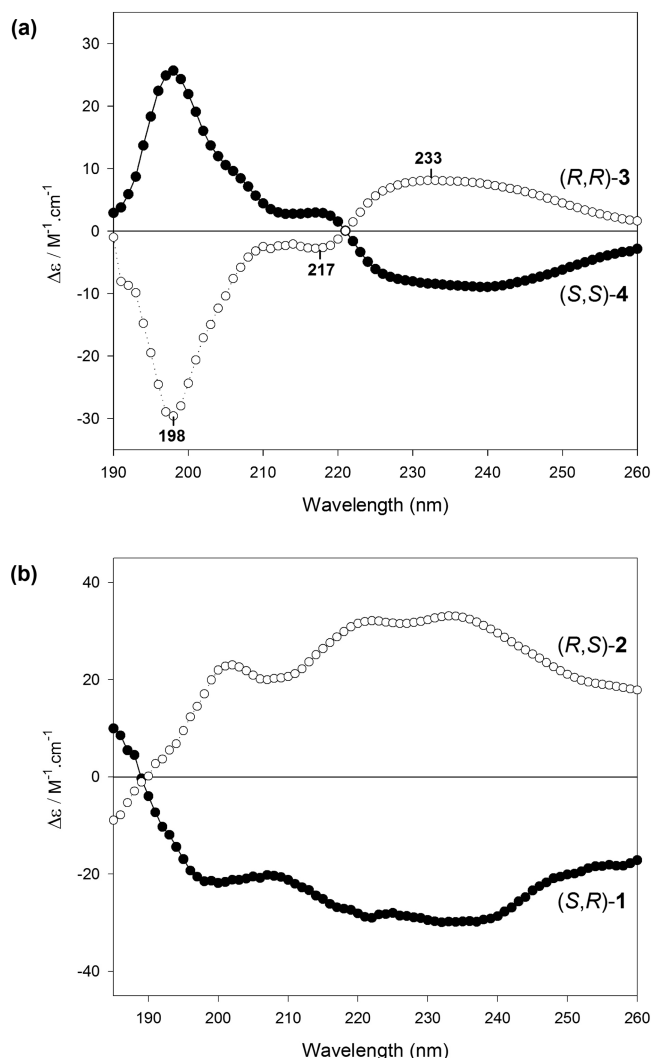


Figure 11. Microcrystalline normalized CD spectra of pseudodipeptides 1–4, in Nujol mulls ($c = 25\text{--}50\text{ mg mL}^{-1}$), in 0.01 cm quartz flat cells, at 293 K; Nujol blank was subtracted from the spectra: (a) Superimposition of homochiral compounds (*R,R*)-3 and (*S,S*)-4 CD spectra. (b) Superimposition of heterochiral compounds (*S,R*)-1 and (*R,S*)-2 CD spectra.

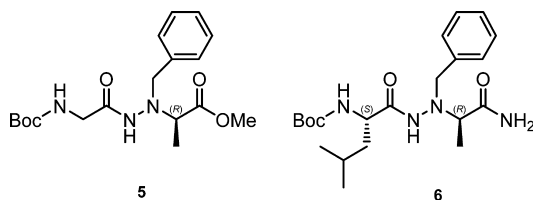


Figure 12. Chemical structure of pseudodipeptides 5 and 6.

enantiomers (1/2 and 3/4). For the concentration dependence experiment in CDCl_3 , the chemical shift of each NH proton was measured under four different concentrations (10^{-4} , 10^{-3} , 10^{-2} , and 10^{-1} M). For the solvent dependence experiment, the chemical shift of each NH proton was measured at a 10^{-2} M concentration at various percentages of $\text{DMSO-}d_6$ in CDCl_3 (0, 0.625, 1.25, 2.5, 5, and 10%).

FTIR Absorption. Infrared spectra were recorded with an attenuated total reflectance Fourier transform infrared (FTIR) spectrophotometer equipped with mid-IR source, KBr beamsplitter, and a liquid-nitrogen-cooled midband mercury cadmium telluride (LN-MCT Narrow) detector. Each spectrum was recorded over 256 scans at 298 K and obtained in CDCl_3 ($c = 10^{-2}$ M) with a CaF_2 cell of

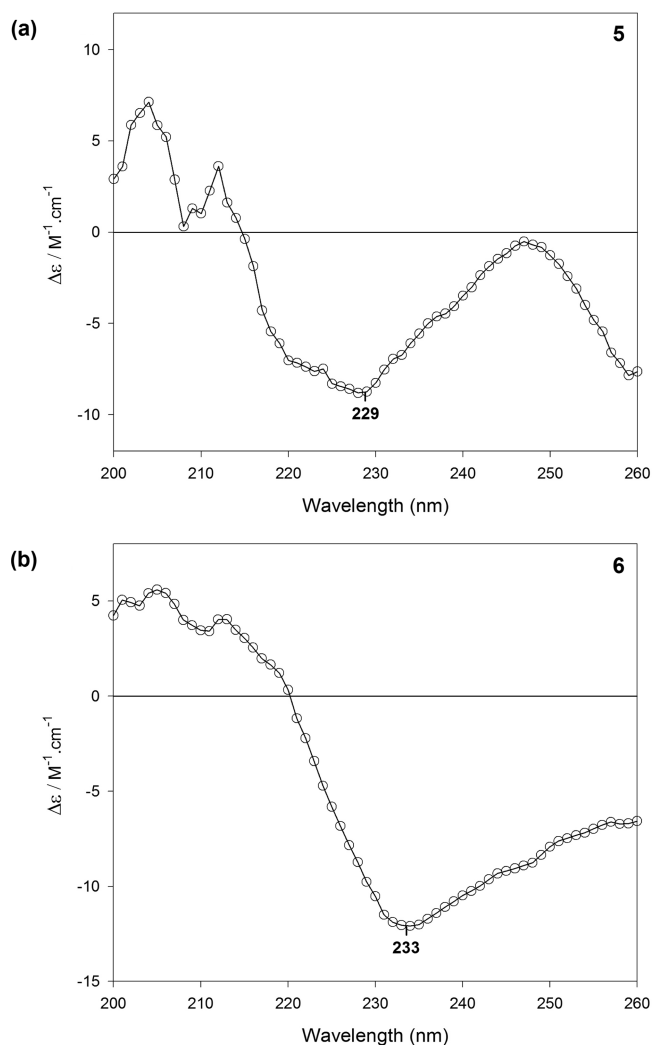


Figure 13. Microcrystalline normalized CD spectra of pseudodipeptides 5 (a) and 6 (b), in Nujol mulls ($c = 50\text{ mg mL}^{-1}$), in 0.01 cm quartz flat cells, at 293 K; Nujol blank was subtracted from the spectra.

500 μm path length at a concentration of 10 mM after subtraction of the solvent spectrum (CDCl_3).

The deconvolution method was used to resolve the overlapping bands in the NH and C=O stretching regions, and the resulting deconvoluted spectra provided information about the conformational equilibrium occurring in the CDCl_3 solution. The deconvolution of N–H and C=O stretching region bands ($3500\text{--}3200\text{ cm}^{-1}$ and $1800\text{--}1600\text{ cm}^{-1}$, respectively) was performed with a software package. Band positions were determined based on fixed number bands obtained from the second derivatives of the original spectra. These bands were automatically adjusted by the damped least-squares optimization algorithm developed by Levenberg–Marquardt. The obtained root-mean-square error (RMSE) was below 0.0009 for each spectrum.

Circular Dichroism. Microcrystalline CD spectra were recorded on a CD spectropolarimeter, scanned on the far-UV range, at 293 K with 1 nm steps from 260 to 190 nm and averaged over three scans. Between each scan, a delay of 5 min was respected to detect any UV-induced modification.²⁹ For each compound, no spectra shape modification was noted. Crystals were crushed with a mortar to obtain a very small granulation, and the microcrystals were then suspended in Nujol oil at a final concentration of 25 or 50 mg mL^{-1} . This preparation provided an optimum homogeneity of Nujol mull, allowing to avoid depolarization or scattering effects.³⁰ Absorbance was simultaneously registered and checked for any variation between

isomers. Moreover, to demonstrate the absence of detectable artifactual signals,³¹ several measurements were performed with different angles by inverting engraved 0.01 cm path length cells by a 180° flip on the y -axis and 90° rotations on the z -axis. With these control conditions, all measurements remained unchanged, providing similar spectra. Absorbance levels, below 1.5 AU, between heterochiral and then homochiral compounds, were superimposable with each other. Nujol is a mixture of hydrocarbons and exhibits significant absorbance below 200 nm. The CD spectra of pure Nujol oil as a function of mdeg and high tension (HT) in the wavelength range from 180 to 260 nm have been recorded to prove the reliability of our CD measurements (see Supporting Information pp S25).

X-ray Diffraction. Crystals of compounds 1–4 exhibited weak diffracting intensities. Their X-ray data were collected at 100 K with a diffractometer equipped with a copper microsource ($\lambda = 1.54184 \text{ \AA}$) and a CCD detector. The structure was solved by direct methods with SIR2014.³² The structure models refinements were conducted using a spherical atom model with ShelXle.³³ All X-ray data for each compound (1–4) are deposited in the CCDC database under access numbers: 1447540, 1447541, 1447542, and 1447543, respectively. Selected crystallographic data for 1–4 are provided in the Supporting Information.

HRMS. The ESI-HRMS analysis was conducted using a quadrupole-time-of-flight (QTOF) mass spectrometer equipped with an ion funnel ESI Electrospray source (1 μL to 1 mL/min).

Characterization of Compounds 1–4. Compounds 1–6 were prepared according to ref 14.

Heterochiral Pseudodipeptides Boc-[(L)-Leucine- α -N^z-benzyl-(D)-hydrazinoalanine]-OMe and Boc-[(D)-Leucine- α -N^z-benzyl-(L)-hydrazinoalanine]-OMe, (S,R)-1 and (R,S)-2. White powder (3.63 g, 96%). Characterization data: mp 111–113 °C; ¹H NMR (300 MHz, CDCl₃, 10 mM) of major conformer δ 0.89 (d, 6H, $J = 6.3 \text{ Hz}$, 2 $\delta\text{CH}_3\text{Leu}$), 1.23–1.65 (m, 6H, $\beta\text{CH}_3\text{Ala}$, $\beta\text{CH}_2\text{Leu}$, γCHLeu), 1.47 (s, 9H, Boc), 3.72–3.83 (m, 1H, αCHAla), 3.78 (s, 3H, OCH₃), 3.88–4.13 (m, 3H, CH₂, N^z-Bn, αCHLeu), 4.77 (br s, NHBoc), 7.23–7.43 (m, 5H, Ar), 7.98 (s, 1H, NH hydrazidic); ¹³C NMR (75 MHz, CDCl₃) of major conformer δ 16.3 ($\beta\text{CH}_3\text{Ala}$), 22.7 (2 $\delta\text{CH}_3\text{Leu}$), 24.6 (γCHLeu), 28.3 (3 CH₃, Boc), 41.2 ($\beta\text{CH}_2\text{Leu}$), 51.6 (O–CH₃), 52.3 (αCHLeu), 60.0 (αCHAla), 60.1 (CH₂, N^z-Bn), 79.9 (C, Boc), 127.6 (CH, Ar), 128.3 (2 CH, Ar), 129.3 (2 CH, Ar), 136.3 (C, Ar), 155.3 (C=O, Boc), 171.1 (C=O, hydrazidic), 174.6 (C=O, ester); HRMS (ESI) calculated for C₂₂H₃₅N₃O₅ [M + H]⁺ m/z 422.2655, found 422.2649 and 422.2646.

Homochiral Pseudodipeptides Boc-[(D)-Leucine- α -N^z-benzyl-(D)-hydrazinoalanine]-OMe and Boc-[(L)-Leucine- α -N^z-benzyl-(L)-hydrazinoalanine]-OMe, (R,R)-3 and (S,S)-4. White powder (3.03 g, 80%). Characterization data: mp 82–84 °C; ¹H NMR (300 MHz, CDCl₃, 10 mM) of major conformer δ 0.94 (d, 6H, $J = 6.3 \text{ Hz}$, 2 $\delta\text{CH}_3\text{Leu}$), 1.34–1.56 (m, 6H, $\beta\text{CH}_3\text{Ala}$, $\beta\text{CH}_2\text{Leu}$, γCHLeu), 1.43 (s, 9H, Boc), 3.68–3.79 (m, 1H, αCHAla), 3.75 (s, 3H, OCH₃), 3.82–3.93 (m, 1H, αCHLeu), 3.96–4.08 (m, 2H, CH₂, N^z-Bn), 4.80 (br s, NHBoc), 7.23–7.39 (m, 5H, Ar), 7.93 (s, 1H, NH hydrazidic); ¹³C NMR (75 MHz, CDCl₃) of major conformer δ 16.1 ($\beta\text{CH}_3\text{Ala}$), 22.6 (2 $\delta\text{CH}_3\text{Leu}$), 24.4 (γCHLeu), 28.3 (3 CH₃, Boc), 41.1 ($\beta\text{CH}_2\text{Leu}$), 51.6 (O–CH₃), 51.9 (αCHLeu), 60.0 (CH₂, N^z-Bn), 60.2 (αCHAla), 79.7 (C, Boc), 127.6 (CH, Ar), 128.2 (2 CH, Ar), 128.8 (2 CH, Ar), 136.4 (C, Ar), 155.5 (C=O, Boc), 171.4 (C=O, hydrazidic), 174.5 (C=O, ester); HRMS (ESI) calculated for C₂₂H₃₅N₃O₅ [M + H]⁺ m/z 422.2655, found 422.2633 and 422.2638.

Pseudodipeptide Boc-[Glycine- α -N^z-benzyl-(D)-hydrazinoalanine]-OMe, 5. Amorphous solid (3.18 g, 97%). Characterization data: ¹H NMR (300 MHz, CDCl₃, 10 mM) δ 1.36–1.44 (m, 12H), 3.57–3.65 (m, 3H), 3.73 (s, 3H), 3.99–4.13 (m, 2H), 5.15 (br s, 1H), 7.26–7.39 (m, 5H), 7.56 (s, 1H); ¹³C NMR (75 MHz, CDCl₃) δ 16.0 (CH₃), 28.2 (CH₃), 41.3 (CH₂), 51.7 (CH₃), 59.7 (CH), 61.9 (CH₂), 79.8 (C), 127.5 (CH), 127.8 (2 CH), 129.1 (2 CH), 135.1 (C), 155.5 (C=O), 172.3 (C=O), 174.2 (C=O); HRMS (ESI) calculated for C₁₈H₂₇N₃O₅ [M + H]⁺ m/z 366.2023, found 366.1998.

Heterochiral Pseudodipeptide Boc-[(L)-Leucine- α -N^z-benzyl-(D)-hydrazinoalanine]-NH₂, 6. White powder (3.45 g, 95%). Character-

ization data: mp 149–151 °C; ¹H NMR (300 MHz, CDCl₃, 10 mM) δ 0.77 (d, 3H, $J = 6.5 \text{ Hz}$), 0.80 (d, 3H, $J = 6.5 \text{ Hz}$), 1.35 (d, 3H, $J = 7.1 \text{ Hz}$), 1.45 (s, 9H), 1.40–1.62 (m, 3H), 3.51 (q, 1H, $J = 7.1 \text{ Hz}$), 3.79–4.03 (m, 3H), 4.69 (br d, 1H, $J = 7.5 \text{ Hz}$), 5.32 (s, 1H), 7.26–7.38 (m, 6H), 8.06 (br s, 1H). The physical data (NMR and HRMS) are in agreement with our values reported in ref 14.

■ ASSOCIATED CONTENT

Supporting Information

The Supporting Information is available free of charge on the ACS Publications website at DOI: 10.1021/acs.joc.6b01680.

Crystallographic file of compound 1 (CIF)

Crystallographic file of compound 2 (CIF)

Crystallographic file of compound 3 (CIF)

Crystallographic file of compound 4 (CIF)

Copies of ¹H NMR and ¹³C NMR spectra of compounds 1–5. Copy of ¹H NMR spectrum of compound 6.

Copies of 2D HSQC and HMBC NMR spectra of compounds 1–4. Concentration and solvent dependence

¹H NMR spectra of compounds 2–4. IR spectra and deconvoluted IR spectra in CDCl₃ of compounds 2–4. IR spectra in MeOH and toluene of compound 1.

Crystallographic data of compounds 1–4. Copies of far UV CD spectra of pure Nujol oil as a function of mdeg and high tension (HT) in the wavelength range from 180 to 260 nm (PDF)

■ AUTHOR INFORMATION

Corresponding Authors

*E-mail: Samir.Acherar@univ-lorraine.fr.

*E-mail: Brigitte.Jamart@univ-lorraine.fr.

Notes

The authors declare no competing financial interest.

■ ACKNOWLEDGMENTS

The authors acknowledge Dr. R. H. Dodd for the critical reading of the manuscript, the DISCO Beamline in Synchrotron “Soleil” for giving us the opportunity to perform SRCD experiments, the SCBIM (Service Commun de Biophysique Interactions Moléculaires) of the Université de Lorraine (FR 3209) for CD experiments and analysis, the experimental platform (Service Commun) of X-ray diffraction of the Institut Jean Barriol for X-ray diffraction analysis, and Mr. O. Fabre for running NMR experiments. This work has been supported by the “Ministère de l’Enseignement Supérieur et de la Recherche” through the Doctoral fellowship of Ms. Eugénie Romero.

■ REFERENCES

- (1) (a) Lehn, J. M. *Science* **1993**, *260*, 1762. (b) Whitesides, G. M.; Mathias, J. P.; Seto, C. T. *Science* **1991**, *254*, 1312. (c) Ball, P. *Nature* **1994**, *369*, 301.
- (2) (a) Taubes, G. *Science* **1996**, *271*, 1493. (b) Baumeister, R.; Eimer, S. *Angew. Chem., Int. Ed.* **1998**, *37*, 2978.
- (3) (a) Goedert, M.; Spillantini, M. G.; Davies, S. W. *Curr. Opin. Neurobiol.* **1998**, *8*, 619. (b) Spillantini, M. G.; Crowther, R. A.; Jakes, R.; Hasegawa, M.; Goedert, M. *Proc. Natl. Acad. Sci. U. S. A.* **1998**, *95*, 6469.
- (4) Koo, E. H.; Lansbury, P. T., Jr.; Kelly, J. W. *Proc. Natl. Acad. Sci. U. S. A.* **1999**, *96*, 9989.
- (5) Cheguillaume, A.; Salaün, A.; Sinbandhit, S.; Potel, M.; Gall, P.; Baudy-Floc’h, M.; Le Grel, P. *J. Org. Chem.* **2001**, *66*, 4923.

- (6) Example for hydrazinopeptides as protease-resisting pseudopeptides: Amour, A.; Collet, A.; Dubar, C.; Reboud-Ravaux, M. *Int. J. Pept. Protein Res.* **1994**, *43*, 297.
- (7) (a) Seebach, D.; Ciceri, P. E.; Overhand, M.; Jaun, B.; Rigo, D.; Oberer, L.; Hommel, U.; Amstutz, R.; Widmer, H. *Helv. Chim. Acta* **1996**, *79*, 2043. (b) Sifferlen, T.; Rueping, M.; Gademann, K.; Jaun, B.; Seebach, D. *Helv. Chim. Acta* **1999**, *82*, 2067. (c) Abele, S.; Seebach, D. *Eur. J. Org. Chem.* **2000**, *2000*, 1. (d) Gademann, K.; Ernst, M.; Seebach, D.; Hoyer, D. *Helv. Chim. Acta* **2000**, *83*, 16 and references cited therein..
- (8) (a) Appella, D. H.; Christianson, L. A.; Karle, I. L.; Powell, D. R.; Gellman, S. H. *J. Am. Chem. Soc.* **1996**, *118*, 13071. (b) Appella, D. H.; Christianson, L. A.; Klein, D. A.; Richards, M. R.; Powell, D. R.; Gellman, S. H. *J. Am. Chem. Soc.* **1999**, *121*, 7574. (c) Barchi, J. J., Jr.; Huang, X.; Appella, D. H.; Christianson, L. A.; Durell, S. R.; Gellman, S. H. *J. Am. Chem. Soc.* **2000**, *122*, 2711. (d) Chung, Y. J.; Huck, B. R.; Christianson, L. A.; Stanger, H. E.; Krausthäuser, S.; Powell, D. R.; Gellman, S. H. *J. Am. Chem. Soc.* **2000**, *122*, 3995 and references cited therein..
- (9) (a) Horne, W. S.; Stout, C. D.; Ghadiri, M. R. *J. Am. Chem. Soc.* **2003**, *125*, 9372. (b) Seebach, D.; Matthews, J. L.; Meden, A.; Wessels, T.; Baerlocher, C.; McCusker, L. B. *Helv. Chim. Acta* **1997**, *80*, 173.
- (10) (a) Pils, L. K. A.; Reiser, O. *Amino Acids* **2011**, *41*, 709. (b) Sharma, G. V. M.; Chandramouli, N.; Choudhary, M.; Nagendar, P.; Ramakrishna, K. V. S.; Kunwar, A. C.; Schramm, P.; Hofmann, H.-J. *J. Am. Chem. Soc.* **2009**, *131*, 17335. (c) Horne, W. S.; Gellman, S. H. *Acc. Chem. Res.* **2008**, *41*, 1399. (d) Roy, A.; Prabhakaran, P.; Baruah, P. K.; Sanjayan, G. J. *Chem. Commun.* **2011**, *47*, 11593. (e) Vasudev, P. G.; Chatterjee, S.; Shamala, N.; Balaram, P. *Acc. Chem. Res.* **2009**, *42*, 1628.
- (11) (a) Guo, L.; Almeida, A. M.; Zhang, W.; Reidenbach, A. G.; Choi, S. H.; Guzei, I. A.; Gellman, S. H. *J. Am. Chem. Soc.* **2010**, *132*, 7868. (b) Karle, I. L.; Pramanik, A.; Banerjee, A.; Bhattacharjya, S.; Balaram, P. *J. Am. Chem. Soc.* **1997**, *119*, 9087. (c) Sharma, G. V. M.; Babu, B. S.; Ramakrishna, K. V. S.; Nagendar, P.; Kunwar, A. C.; Schramm, P.; Baldauf, C.; Hofmann, H.-J. *Chem. - Eur. J.* **2009**, *15*, 5552.
- (12) (a) Steer, D. L.; Lew, R. A.; Perlmutter, P.; Smith, A. I.; Aguilar, M.-I. *Curr. Med. Chem.* **2002**, *9*, 811. (b) Guichard, G.; Zerbib, A.; Le Gal, F. A.; Hoebeke, J.; Connan, F.; Choppin, J.; Briand, J. P.; Guillet, J. G. *J. Med. Chem.* **2000**, *43*, 3803.
- (13) Marraud, M.; Vanderesse, R. R. In *Houben-Weyl: Methods of Organic Chemistry*; Goodman, M.; Felix, A.; Moroder, L.; Toniolo, C., Eds.; Thieme: Stuttgart, Germany, 2003; Vol. E22c, pp 423–457.
- (14) Moussodia, R.-O.; Acherar, S.; Bordessa, A.; Vanderesse, R.; Jamart-Grégoire, B. *Tetrahedron* **2012**, *68*, 4682.
- (15) Moussodia, R.-O.; Acherar, S.; Romero, E.; Didierjean, C.; Jamart-Grégoire, B. *J. Org. Chem.* **2015**, *80*, 3022.
- (16) (a) Koh, J. T.; Cornish, V. W.; Schultz, P. G. *Biochemistry* **1997**, *36*, 11314. (b) Chapman, E.; Thorson, J. S.; Schultz, P. G. *J. Am. Chem. Soc.* **1997**, *119*, 7151. (c) Shin, I.; Ting, A. Y.; Schultz, P. G. *J. Am. Chem. Soc.* **1997**, *119*, 12667. (d) Deechongkit, S.; Dawson, P. E.; Kelly, J. W. *J. Am. Chem. Soc.* **2004**, *126*, 16762.
- (17) Lecoq, A.; Marraud, M.; Aubry, A. *Tetrahedron Lett.* **1991**, *32*, 2765.
- (18) (a) Pispisa, B.; Stella, L.; Venanzi, M.; Palleschi, A.; Polese, A.; Formaggio, F.; Toniolo, C. *J. Pept. Res.* **2000**, *56*, 298. (b) Roy, R. S.; Karle, I. L.; Raghothama, S.; Balaram, P. *Proc. Natl. Acad. Sci. U. S. A.* **2004**, *101*, 16478. (c) Rai, R.; Raghothama, S.; Balaram, P. *J. Am. Chem. Soc.* **2006**, *128*, 2675. (d) Chang, X.-W.; Han, Q.-C.; Jiao, Z.-G.; Weng, L.-H.; Zhang, D. W. *Tetrahedron* **2010**, *66*, 9733. (e) Donoli, A.; Marcuzzo, V.; Moretto, A.; Crisma, M.; Toniolo, C.; Cardena, R.; Bisello, A.; Santi, S. *Biopolymers* **2013**, *100*, 14. (f) Acherar, S.; Salaün, A.; Le Grel, P.; Le Grel, B.; Jamart-Grégoire, B. *Eur. J. Org. Chem.* **2013**, *2013*, 5603.
- (19) Le Grel, P.; Salaün, A.; Mocquet, C.; Le Grel, B.; Roisnel, T.; Potel, M. *J. Org. Chem.* **2011**, *76* (21), 8756.
- (20) (a) Schrauber, H.; Eisenhaber, F.; Argos, P. *J. Mol. Biol.* **1993**, *230*, 592. (b) MacKenzie, K. R.; Prestegard, J. H.; Engelman, D. M. *J. Biomol. NMR* **1996**, *7*, 256.
- (21) Formaggio, F.; Crisma, M.; Toniolo, C.; Broxterman, Q. B.; Kaptein, B.; Corbier, C.; Saviano, M.; Palladino, P.; Benedetti, E. *Macromolecules* **2003**, *36*, 8164.
- (22) For example, see: Jacobsen, O.; Gebreslasie, H. G.; Klaveness, J.; Rongved, P.; Görbitz, C. H. *Acta Crystallogr., Sect. C: Cryst. Struct. Commun.* **2011**, C67, o278 and the references mentioned therein..
- (23) Oku, H.; Yamada, K.; Katakai, R. *Biopolymers* **2008**, *89*, 270.
- (24) Formaggio, F.; Moretto, A.; Crisma, M.; Toniolo, C. in *Peptide Materials from Nanostructures to Applications*; Alemán, C.; Bianco, A.; Venanzi, M., Eds.; John Wiley & Sons: Hoboken, NJ, 2013; Chapt. 2, pp 39–63.
- (25) Wen, L.-R.; Liu, P.; Li, M. *Acta Crystallogr., Sect. E: Struct. Rep. Online* **2007**, *63*, o1212.
- (26) (a) Castiglioni, E.; Biscarini, P.; Abbate, S. *Chirality* **2009**, *21*, E28. (b) Kuroda, R.; Harada, T. In *Comprehensive Chiroptical Spectroscopy, Instrumentation, Methodologies, and Theoretical Simulations*; Berova, N.; Polavarapu, P. L.; Nakanishi, K.; Woody, R. W., Eds.; John Wiley & Sons: Hoboken, NJ, 2012; Chapter 4, pp 91–113.
- (27) Greenfield, N.; Fasman, G. D. *Biochemistry* **1969**, *8*, 4108.
- (28) Pescitelli, G.; Di Pietro, S.; Cardellicchio, C.; Capozzi, M. A. M.; Di Bari, L. *J. Org. Chem.* **2010**, *75*, 1143.
- (29) Hariu, N.; Ito, M.; Akitsu, T. *Contemp. Eng. Sci.* **2015**, *8*, 57.
- (30) (a) Kuroda, R. In *Circular Dichroism: Principles and Applications*, 2nd ed.; Berova, N.; Nakanishi, K.; Woody, R. W., Eds.; John Wiley & Sons: Hoboken, NJ, 2000; pp 159–184. (b) Kuroda, R. Ph.D. Thesis, University of Tokyo, 1975.
- (31) (a) *Comprehensive Chiroptical Spectroscopy, Applications in Stereochemical Analysis of Synthetic Compounds, Natural Products, and Biomolecules*; Berova, N.; Prasad, L.; Polavarapu; Nakanishi, K.; Woody, R. W., Eds.; John Wiley & Sons: Hoboken, NJ, 2012. (b) Kuroda, R.; Harada, T.; Shindo, Y. *Rev. Sci. Instrum.* **2001**, *72*, 3802. (c) Pescitelli, G.; Kurtán, T.; Flörke, U.; Krohn, K. *Chirality* **2009**, *21*, E181.
- (32) Burla, M. C.; Caliandro, R.; Carrozzini, B.; Cascarano, G. L.; Cuocci, C.; Giacovazzo, C.; Mallamo, M.; Mazzone; Polidori, G. *J. Appl. Crystallogr.* **2015**, *48*, 306.
- (33) Hübschle, C. B.; Sheldrick, G. M.; Dittrich, B. *J. Appl. Crystallogr.* **2011**, *44*, 1281.